SPATIAL TRANSCRIPTOMICS OF THORACIC AORTIC PATHOLOGY

Carla Dominguez Gonzalez, BS; Vainhav Jain, MA; Carolyn Glass, MD, PhD.

a. Dept. of Pathology, Div. of Cardiovascular Pathology, Duke University School of Medicine, Durham, NC; b Duke Molecular Physiology Institute, Duke University School of Medicine, Durham, NC; Biorepository and Precision Pathology Center, Duke University School of Medicine, Durham, NC

INTRODUCTION

- Aortopathies are major life-threatening diseases worldwide, with the incidence and mortality of aortitis, aortic aneurysm and aortic dissection rising in the past decade.
- The cellular and molecular drivers of aortic pathology are not fully elucidated, which hinders prevention, diagnosis and treatment.

- Spatially resolved transcriptomic technologies are unlocking novel insights into tissue biology.
- They can measure gene expression with spatial context, and thus, map the organization of cell types, define their molecular characteristics and uncover the interactions amongst populations.

STUDY OBJECTIVE

To create a combined molecular-histologic map at the whole transcriptome level of common human aortic pathologies with the goal of identifying pathologic cell populations and their molecular signature.

METHODS

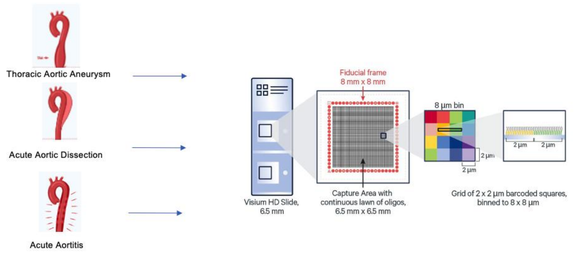

Figure 1. Tissue Preparation. Using human aortic tissue from three separate subjects who underwent repair for an enlarging thoracic aortic aneurysm, acute aortic dissection and acute aortitis FFPE tissue slides where prepared on Visium HD slides.

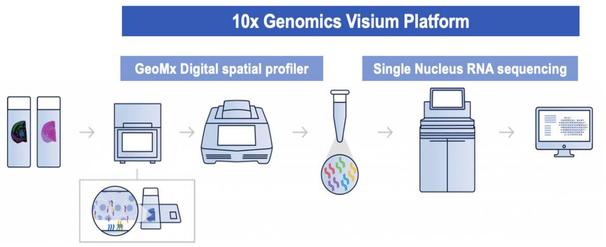

Figure 2. Spatial Transcriptomics model. Aortic Tissue was processed through the 10x Genomics Visium platform using the GeoMx digital spatial profiler and single-nucleus RNA sequencing were completed to identify gene expression signatures within single cells and map distinct cellular populations.

FIGURE 3. SnRNA Spatial Transcriptomics Reveal Distinct Cell Sub-Population within pathologic aortic layer

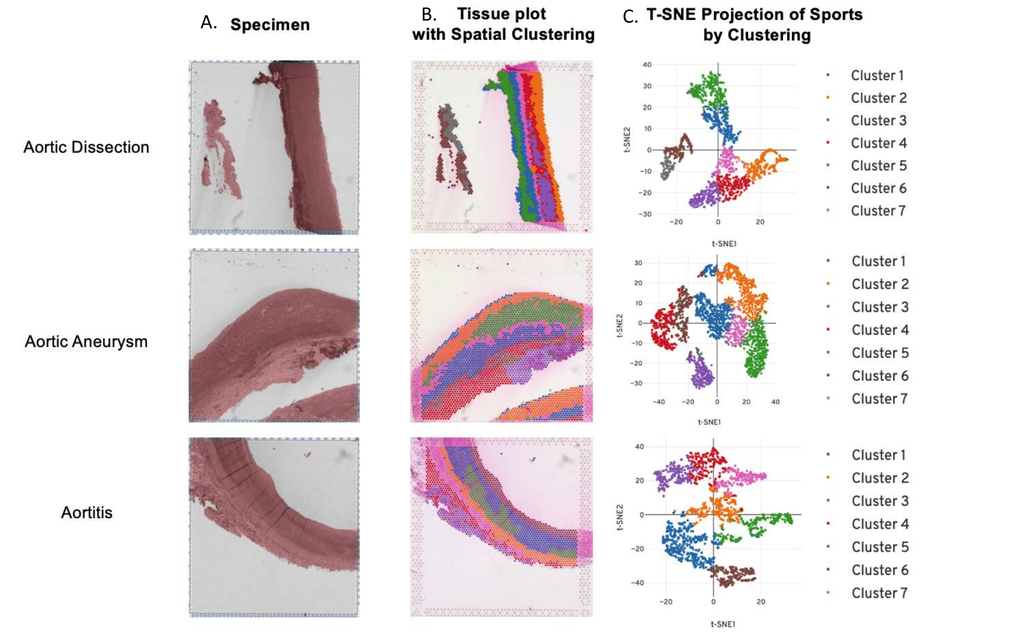

Figure 1. A)High Resolution FFPE Human Aortic Specimen tissue section. B) Spatially resolved distribution of differentially expressed clusters across pathology specimen, colored by cluster, identifies distinct cell population characteristics within each aortic layer. C) t-Distributed Stochastic Neighbor Embedding (t-SNE) plot of cell clusters found, Cell clustering based on differential gene expression

Figure 4. UMI differential comprehensive expression analysis

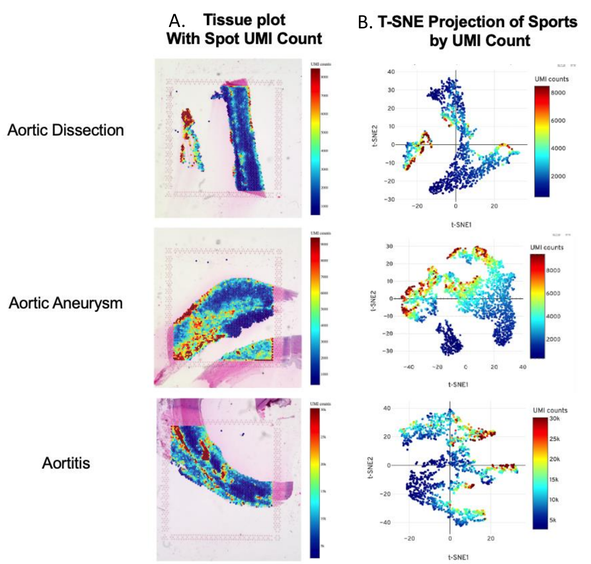

Figure 1. A) Spatially resolved UMI (unique molecular identifier) count per reading spot, plot showing transcript count per fov in each sample. Each fov is 200 µm. Higher UMI count correlated with increased transcription activity. B) t-SNE plot of reading spots colored by UMI count.

Table 1. Top 5 Most Differentially expressed Genes by Cluster

	Aortic Dissection		Aortic Aneurysm		Aortitis	
Cluster 1	Gene	P-value	Gene	P-value	Gene	P-value
	IGFBP3	2.8601E-60	*APOD*	6.286E-230	HSPB7	2.574E-142
	C3	1.9841E-53	*GPHA2*	2.758E-211	SUSD5	5.089E-135
	FLNC	2.4936E-52	*CFD*	4.409E-202	SOST	5.882E-126
	PLAT	2.7402E-50	*C3*	4.341E-199	RAMP1	1.066E-113
	CRYAB	9.2681E-49	*CXCL14*	1.38E-170	TPM2	1.104E-112
Cluster 2	*ADH1B*	3.2693E-80	*PI16*	1.60E-216	COMP	3.277E-120
	S100A8	3.1165E-73	*PLA2G2A*	4.63E-190	LRRC15	8.547E-58
	S100A9	5.6544E-61	*FBLN1*	7.650E-187	CRTAC1	4.085E-50
	LMOD1	9.7635E-59	*DCN*	1.591E-183	SERPINE2	1.025E-48
	FMO2	5.2795E-58	*C7*	1.591E-193	COL10A1	1.322E-33
Cluster 3	*HBA2*	1.848E-43	C3	3.181E-86	MMP12	1.711E-224
	HBB	3.0958E-38	CARTPT	1.542E-82	SPP1	1.589E-213
	CXCL5	2.517E-26	CFD	6.185E-80	TREM1	7.658E-204
	PPBP	2.3962E-24	APOD	5.3686E-77	MT1H	3.300E-200
	MARCO	1.1911E-22	IGFBP4	1.456E-75	MT1G	1.203E-195
Cluster 4	*EGLN3*	1.1968E-29	APOD	0	PLIN1	6.495E-71
	S100A9	2.5641E-28	FABP4	0	FABP4	4.260E-69
	COL13A1	1.7207E-26	MYH10	0	SPP1	7.258E-69
	SNCG	8.1743E-23	TNFRSF11B	6.852E-234	PLIN4	1.349E-67
	SLC2A1	8.4063E-23	CFD	3.346E-231	ADIPOQ	3.857E-63
Cluster 5	*EGLN3*	2.1344E-13	HBA2	2.292E-85	LYVE1	1.431E-113
	SNCG	2.1344E-13	HBB	6.612E-72	THBS4	3.585E-104
	SLC2A1	1.9491E-10	HBD	8.909E-34	TNXB	4.511E-86
	THBS2	2.7001E-10	MT-ND5	1.926E-21	MFAP5	1.767E-80
	COL13A1	5.6384E-10	MT-ND3	1.2461E-19	IL6	2.286E-80
Cluster 6	*DEPP1*	3.1563E-84	PI16	3.309E-126	CRLF1	8.072E-135
	TPM2	2.6418E-83	THBS4	4.685E-105	IGFBP3	3.636E-123
	APOD	6.0196E-78	SFRP2	1.112E-100	FMO3	1.092E-113
	CFD	7.809E-73	CCDC80	7.2139E-85	PLA2G2A	1.511E-102
	FN1	1.3002E-71	SERPINE2	5.303E-77	CDH2	9.857E-97
Cluster 7	*CARTPT*	2.0984E-20	C3	1.773E-43	MS4A1	2.427E-208
	S100A9	7.8588E-15	APOD	2.477E-38	IGHD	6.789E-205
	S100A8	3.2781E-14	DCN	4.129E-37	BLK	1.197E-194
	EGLN3	6.7525E-12	CFD	1.472E-35	NIBAN3	1.073E-187
	FCER1G	6.8254E-12	SFRP2	1.076E-33	CXCL13	1.766E-186

RESULTS

Figure 5. Heat Map of Top 100 Genes Expressed: Clusters Composing Aortic Medial Layer

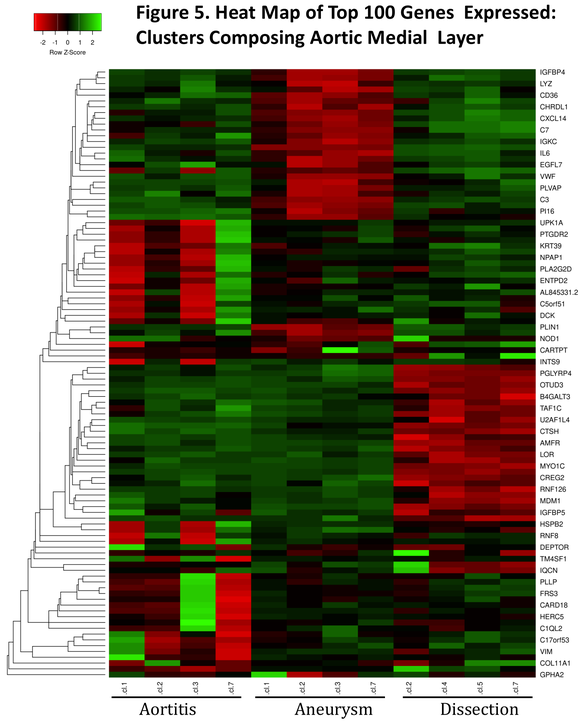

CONCLUSIONS

- We provide a novel combined molecular-histologic map at the whole transcriptome level of common human aortic pathologies.
- Spatial transcriptomics provides insight about the relationship between dimensional tissue organization and dysregulated molecular networks that may be pathologic hallmarks in specific cellular populations
- These findings may facilitate discovery of future novel interventional targets with direct functional relevance for the diagnosis and treatment of thoracic aortic diseases.

REFERENCES

Han Y et al. Histone acetylation and histone acetyltransferases show significant alterations in human abdominal aortic aneurysm. 2016
Jones et al. Meta-analysis of genome-wide association studies for abdominal aortic aneurysm identifies four new disease-specific risk loci. 2017
Toghill BJ Et al. Smyd2 promoter DNA methylation is associated with abdominal aortic aneurysm (aaa) and smyd2 expression in vascular smooth muscle cells. 2018

Louis Saddic, Amanda Orosco, Dongchuan Guo, Dianna M. Milewicz, Dana Troxlair, Richard Vander Heide, David Herrington, Yue Wang, Ali Azizzadeh, Sarah J. Parker,

Shireman PK, McCarthy WJ, Pearce WH, Shively VP, Cipollone M, Kwaan HC. Elevations of tissue-type plasminogen activator and differential expression of urokinase-type plasminogen activator in diseased aorta. J Vasc Surg. 1997 Jan;25(1):157-64

Yang L, et al Alpha-crystallin B chains enhance cell migration in basal-like 2 triple-negative breast cancer cells.. Pharmazie, 2022 Feb 1. PMID 35209962

Proteomic analysis of descending thoracic aorta identifies unique and universal signatures of aneurysm and dissection,JVS-Vascular Science,Volume 3,2022. Pages 85-181,

Chen S, Chen H, Zhong Y, Ge Y, Li C, Qiao Z, Zhu J. Insulin-like growth factor-binding protein 3 inhibits angiotensin II-induced aortic smooth muscle cell phenotypic switch and matrix metalloproteinase expression. Exp Physiol. 2020 Nov;105(11):1827-1839.

Kang, BE et al. Epigenetic modulation in the pathogenesis and treatment of inherited aortic aneurysm conditions. 2021